Strojniški vestnik - Journal of Mechanical Engineering 68(2022)10, 635-641
DOI:10.5545/sv-jme.2022.222
Short Scientific Paper
Received for review: 2022-06-20
Received revised form: 2022-09-08
Accepted for publication: 2022-09-09

Thermal Evaluation of Multilayer Wall with a Hat-Stringer in Aircraft Design

Volodymyr Brazhenko[1,2] – Yibo Qiu[1] – Jiancheng Cai[1,2,*] – Dongyun Wang[1,2]

[1] Zhejiang Normal University, College of Engineering, China
[2] Zhejiang Normal University, Key Laboratory of Urban Rail Transit Intelligent Operation and Maintenance Technology & Equipment of Zhejiang Province, China

In the present paper, we investigate the heat transfer through the multilayer wall of aircraft cabins, as this process influences the comfortable conditions created for most passengers and crew members. The numerical modelling results and calculation of a multilayer wall with a hat-stringer in aircraft design are presented. The thermal characteristics evaluation and their relationship with the design parameters were made. The effect of the air layer size on the overall thermal resistance of the multilayer wall, taking into account the geometrical dimensions and properties of the surfaces, was studied. The relative temperature field in the insulation layer, which crosses the hat-stringer elements of the fuselage frame, is calculated. It is shown that the insufficient thickness of the layer of thermal insulation material in the zone of the hat-stringer at low temperatures leads to a significant deterioration in the multilayer wall characteristics, which can worsen the microclimatic conditions inside the aircraft cabin.

Keywords: numerical modelling, heat transfer, aircraft design, multilayer wall, hat-stringer

Highlights

- *The air layer thickness, up to which the thermal resistance of the multilayer wall increases, was determined.*
- *The relationship between the size of the insulating material and the heat transfer coefficient was obtained.*
- *The effect of a hat-stringer on the thermal characteristics of a multilayer wall of an aircraft cabin was evaluated.*

0 INTRODUCTION

Nowadays, the civil aircraft industry faces a variety of challenges and demands, including ensuring a comfortable environment for passengers on board aircraft. In the rational design of present-day passenger aircraft, a heightened level of attention is focused on creating a comfortable condition for travellers and crew members in the aircraft cabin, chiefly by improving the quality of indoor climate conditions [1] to [5]. The core part of an aircraft is the cabin, which provides the necessary environmental conditions for travellers and crew members. The first priority of the cabin is to protect people on board from the harmful effects of the external atmosphere. The second is to ensure that the required pressure, temperature, and air composition are maintained on board the aircraft. To shield passengers from aggressive environmental conditions outside the cabin, in particular, from low temperatures outside and to ensure comfortable thermal conditions for humans inside, a specific insulation material and air layer are provided in the construction of the multilayer wall of the aircraft cabin (Fig. 1a). When designing an aircraft, the most significant heat characteristic of the cabin is thermal protection, which can be determined based on the cabin heat exchange with the environment. Insulation material with a very small value of thermal conductivity coefficient is typically utilized in multilayer walls to insulate the aircraft cabin.

Several recent articles on this topic have considered the challenges of providing thermal comfort [6] to [9] and heat transfer in the cabin [10] to [14]. However, the construction of the multilayer cabin wall in the design of aircraft and its influence on the comfortable environment for passengers play a significant role, which is not considered in these papers.

The multilayer wall of an aircraft cabin consists of the outer shell of the fuselage, the insulation layer, and the inner edging. There is an air layer between the edging and the insulation that houses the equipment wires and other hardware (Fig. 1b).

Of particular interest is the intersection of the thermal insulation layer with the stringers of the fuselage frame since the thermal conductivity of the stringers is several orders higher than the thermal conductivity of the insulation [15]. At sufficiently low ambient temperatures outside the aircraft, stringers are good conductors, through which there is significant heat loss that can cause deterioration of the microclimate in the cabin and the appearance of condensation.

The key question that this paper will address is the thermal evaluation of cabin multilayer walls with a hat-stringer, which crosses the insulation layer. It

*Corr. Author's Address: Zhejiang Normal University, 688 Yingbin Road, Jinhua, Zhejiang Province, China, cai_jiancheng@foxmail.com

should be noted that this study can be useful for the comprehensive development of lightweight insulation materials [16] and [17], to study the reduction of moisture accumulation in insulation materials [18], as well as to find new ways to protect the insulation layer from moisture penetration [19] to [21].

1 NUMERICAL MODEL AND SETTINGS

The heat transfer process through a wall consisting of several layers with different thermophysical characteristics and homogeneous properties was analysed. Heat flux through the layer is directed along the normal to external and internal surfaces and contingent only on the temperature difference. Heat transfer through the edging and insulation layer is carried out as a result of the material thermal conductivity, as for the air layer due to thermal conductivity, natural convection, and heat emission. The principle of independent accounting of heat transfer was applied to the air layer. Also, the area with the insulation layer was considered, inside which the hat-stringer is positioned (Fig 1c).

The heat flux density due to heat conduction through the multilayer cabin wall with flat homogeneous layers without internal heat sources: $\partial T/\partial n = dT/dx$, is determined with the Fourier equation:

$$\overline{q} = -\lambda \frac{dT}{dx} = -\frac{\lambda}{\delta}\Delta T, \tag{1}$$

where $\overline{q}$ is the heat flux density vector, λ is the layer thermal conductivity and equals to constant, ΔT is the temperature difference on boundaries of the layer, and δ is the layer thickness. For edging and insulation layers, λ is the thermal conductivity of solid material. In this model, we investigated the thermal resistance of the cabin multilayer wall, which involves an air layer with its specific dimensions and emissivity factor of boundaries. For the air layer, λ_{AL} is the equivalent coefficient of heat transfer by heat conduction and is defined as specified in Eq. (2):

$$\lambda_{AL} = \varepsilon_{AL}\lambda_a + \alpha_{AL}\delta_{AL}, \tag{2}$$

where ε_{AL} is the convection factor to take into account the effect of natural convection on boundaries of air layer (Eq. (3)); λ_a is the thermal conductivity coefficient of air; δ_{AL} is the thickness of an air layer; α_{AL} is the radiation heat transfer coefficient. The coefficient ε_{AL} depends on the temperature difference at the surfaces of the air layer. The value of the coefficient can be determined using Eq. (3):

$$\varepsilon_{AL} = 0.105 \cdot \left(\frac{g\delta_{AL}^{\,3}\left(\frac{(T_e - T_i)}{0.5\cdot(T_e + T_i)+273}\right)}{\nu^2}\mathrm{Pr} \right)^{0.3}, \tag{3}$$

where g is the acceleration of gravity, ν is coefficient of kinematic viscosity of air, δ_{AL} is air layer thickness, T_e, T_i are temperatures on the boundaries of air layer, and Pr is Prandtl numbers (taken up as Pr = 0.7). The radiation heat transfer coefficient is determined according to the following expression:

$$\alpha_{AL} = \frac{C_0\left[\left(\frac{T_e+273}{100}\right)^4 - \left(\frac{T_i+273}{100}\right)^4\right]}{\left(\frac{1}{\varepsilon_e}+\frac{1}{\varepsilon_i}-1\right)(T_e - T_i)} \tag{4}$$

where ε_e and ε_i are the emissivity coefficients of the air layer surfaces; C_0 is the blackbody coefficient.

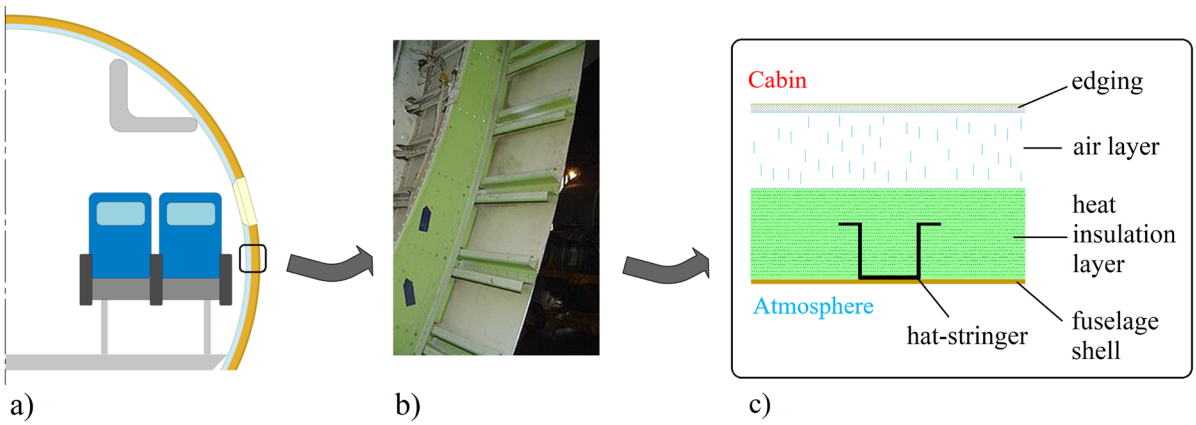

Fig. 1. *Placement of stringers; a) cabin cross-section, b) original fuselage [22], c) fuselage design scheme*

It is necessary to solve a system of equations with unknown temperatures T_i, T_e and total heat flux q to obtain the equation of heat transfer through the multilayer wall of the considered aircraft cabin.

$$\begin{cases} q = \dfrac{\lambda_i}{\delta_i}\left(T_i - T_a\right) \\ q = q_\lambda + q_\alpha + q_\varepsilon = \dfrac{\lambda_{AL}}{\delta_{AL}}\left(T_e - T_i\right), \\ q = \dfrac{\lambda_e}{\delta_e}\left(T_c - T_e\right) \end{cases} \tag{5}$$

where in this system q_λ, q_α, and q_ε are heat fluxes, caused by thermal conductivity, natural convection and heat radiation; δ_i and δ_e are thicknesses of insulation and edging layers; λ_i and λ_e are thermal conductivities of insulation and edging layers; T_a and T_c are temperatures on outside aircraft cabin and air in-cab environment. The change in the amount of heat that passes through a multilayer wall is related to the thermal resistance of each layer. The wall resistance is specified by the geometry configurations and heat properties of the layer material: $r_{full} = \delta_i/\lambda_i + \delta_{AL}/\lambda_{AL} + \delta_e/\lambda_e$; the temperatures T_i and T_e are determined by a solving system of Eq. (5) and taking into account values of Eq. (2) to (4). These temperatures enable determining the equivalent heat transfer coefficient λ_{AL}, and values λ_i and λ_e were taken as constant heat transfer coefficients of corresponding layers.

The thermal emissivity on the fuselage shell of a multilayer wall is mainly determined according to the ambient conditions outside the aircraft cabin. Since the thickness of the layer shell is relatively small and the thermal conductivity of its material has a sufficiently high value, we did not take into account the influence of the thermal resistance of the outer shell on the total resistance in the model. Thus, on the outer surface of the insulation layer, we set the temperature determined from outside of the aircraft cabin. The temperature on the internal surface of the edging can be set according to comfortable thermal conditions for people inside the cabin.

The system of equations in Eq. (5) consists of nonlinear algebraic equations. The exact solution to this system is impossible. Therefore, an approximate iterative method with the control of heat balance in mesh cells was proposed for solutions [22] and [23]. The temperature distribution in all layers and on internal surfaces of the multilayer wall was calculated numerically. The changing of heat transfer characteristics of insulation was estimated in the presence of a hat-stringer inside (Fig. 2). The influence of the air layer parameters on the change in multilayer wall thermal characteristics was investigated.

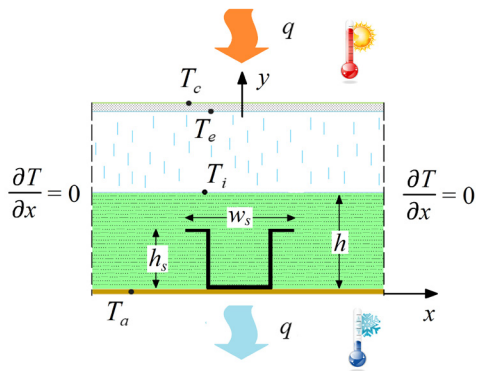

Fig. 2. *Schematic diagram of multilayer wall with hat-stringer in thermal insulation*

The steady-state differential equation of heat conduction in a two-dimensional xy coordinate system has the form:

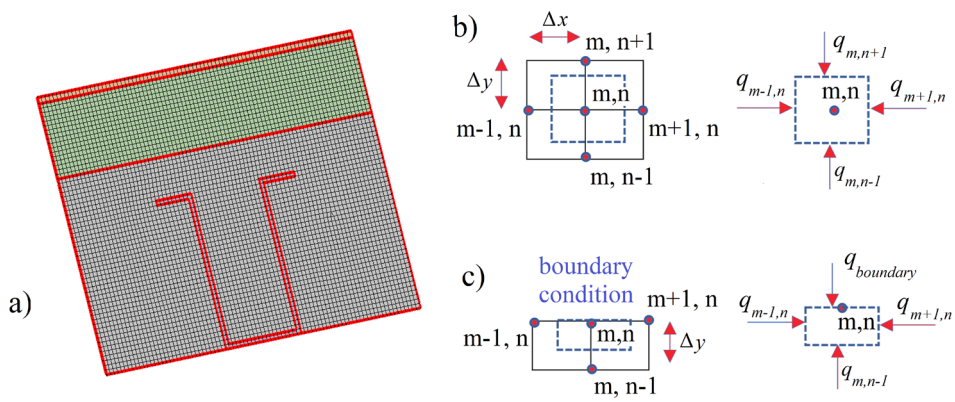

Fig. 3. *Calculation mesh and control cells: a) computational mesh view, b) internal control cell, c) control cell near boundary*

$$\frac{\partial}{\partial x}\left(\lambda\ \frac{\partial T}{\partial x}\right)+\frac{\partial}{\partial y}\left(\lambda\ \frac{\partial T}{\partial x}\right)=0. \qquad (6)$$

The temperature on the external surface of the insulation is set by the temperature outside the aircraft, as noted earlier. Adiabatic conditions $\partial T/\partial x = 0$ are fulfilled at the free boundaries. The boundary condition for the internal surface (e.g., for insulation) is written as:

$$\lambda_i \frac{\partial T}{\partial y} = -\alpha\left(T_{AL} - T_c\ \right). \qquad (7)$$

To solve Eq. (6) with given boundary conditions, we used a numerical method with mesh (Fig. 3a) based on the heat balance equation with the finite-difference approach over the control cell (Fig. 3b):

$$q_{m-1,n} + q_{m+1,n} + q_{m,n-1} + q_{m,n+1} = 0. \qquad (8)$$

The heat flux through the multilayer wall of the cabin can be written by substituting Fourier's Law and the definition of heat rate per unit area for each heat flux node:

$$A_1\left(-\lambda\frac{T_{m,n}-T_{m-1,n}}{\Delta x}\right)+A_2\left(-\lambda\frac{T_{m,n}-T_{m+1,n}}{\Delta x}\right)+$$
$$A_3\left(-\lambda\frac{T_{m,n}-T_{\boldsymbol{m}-1,n}}{\Delta y}\right)+A_4\left(-\lambda\frac{T_{m,n}-T_{m+1,n}}{\Delta y}\right)=0, \qquad (9)$$

where A_1, A_2, A_3 and A_4 are the unit areas; T is the temperature in the corresponding node. Since in computation mesh $\Delta x = \Delta y$ previous equation can be rewritten as with rearranging:

$$4T_{m,n} - T_{m,n+1} - T_{m,n-1} - T_{m+1,n} - T_{m,n-1} = 0\,. \qquad (10)$$

For mesh cell with boundary case (Fig. 3c):

$$4T_{m,n} - 2T_{m,n-1} - T_{m+1,n} - T_{m-1,n} = 0. \qquad (11)$$

In the last step, an augmented matrix $[A|b]$ consisting of temperatures at each node was compiled. The solution of the matrix equation $[A]x = b$, was expressed as $x = [A]^{-1}b$.

2 THERMAL EVALUATION OF MULTILAYER WALL

For the thermal evaluation of the multilayer wall with a hat-stringer, the next modelling constants were adopted: air temperature of atmosphere outside and inside cabin: T_a = –25 °C, T_e = 20 °C; thermal conductivity and thickness of edging and thermal insulation, respectively: λ_e = 0,5 W/(m·°C), λ_i = 0.05 W/(m·°C), $\delta_e = 3\cdot10^{-3}$ m, $\delta_i = 9\cdot10^{-2}$ m. The thermal conductivity in the air layer λ_a was calculated by the average temperature T_{AL} in the air layer. Air layer characteristics were varied for investigation: thickness δ_{AL} in a range from 0 m to $7.5\cdot10^{-2}$ m and emissivity factor of air layer boundaries $\varepsilon_e = \varepsilon_i$ from 0.1 to 0.9. As noted earlier, the aircraft cabin shell can be neglected because of its physical and geometric properties.

Fig. 4 demonstrates a relative thermal resistance of insulation layer $r_i' = r_i / r_{full} \cdot 100$ % and air layer $r_{AL}' = r_{AL} / r_{full} \cdot 100$ %, Fig. 5 shows $\kappa_{full} = 1 / r_{full}$ is the heat transfer coefficient; in Fig. 6, $\lambda_{full} = (\delta_i + \delta_{AL} + \delta_e) / r_{full}$ is the equivalent coefficient of thermal conductivity of cabin multilayer wall.

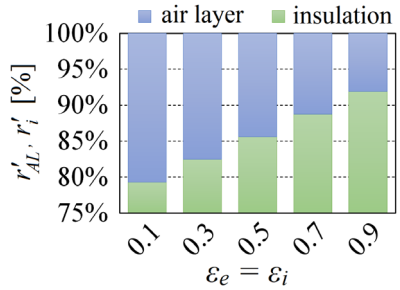

Fig. 4. *Contributions of air layers and insulation in full thermal resistance of multilayer wall (δ_{AL} = 2.9·10⁻² m), for different $\varepsilon_e = \varepsilon_i$*

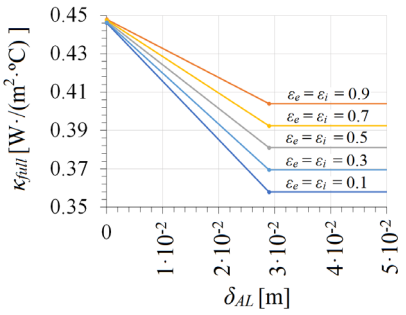

Fig. 5. *Heat transfer coefficient of multilayer wall for different values $\varepsilon_e = \varepsilon_i$*

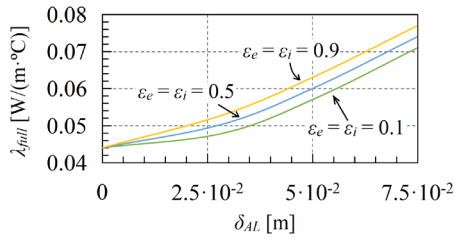

Fig. 6. *Thermal conductivity coefficient of cabin multilayer wall*

The contribution of air layer thermal resistance for different values $\varepsilon_e = \varepsilon_i$ is changing from 20.7 % for $\varepsilon_e = \varepsilon_i$ = 0.1 to 8.1 % for $\varepsilon_e = \varepsilon_i$ = 0.9 from the

total resistance of multilayer wall. According to results in Fig. 5, we may conclude that increasing the thickness of the air layer by more than $2.9 \cdot 10^{-2}$ m does not provide an increase in multilayer wall thermal resistance.

Fig. 7 shows the changing of relative temperature in the insulation of the cabin multilayer wall, in which the hat-stringer is placed. For this, according to Earth's atmosphere conditions, we considered temperature $T_a = -55$ ºC (the atmospheric temperature at an altitude of 11 kilometres), $T_a = -65$ ºC and $T_a = -75$ ºC (minimum temperature, depending on the season). The temperature inside the cabin was taken as $T_c = 20$ ºC; the difference between cabin temperature and internal surfaces $\Delta T_w = T_c - T_w = 5$ ºC; the heat-transfer coefficient of internal surfaces was 8 W/(m²·ºC). The thermal conductivity ratio between of hat-stringer and the thermal insulation was 5500. The relative height of the insulation layer was determined according to the expression: $\overline{h} = w_s/(h - h_s)$ and equals 2.5, 3, or 3.5, respectively. The evaluation of the thermal field for $t_a = -55$ ºC, $\overline{h} = 3.5$ are shown in Fig. 6 in the curves form of constant relative temperature changing $\psi_i = (T_i - T_a)/(T_c - T_a)$, where T_i is the temperature field in the insulation layer.

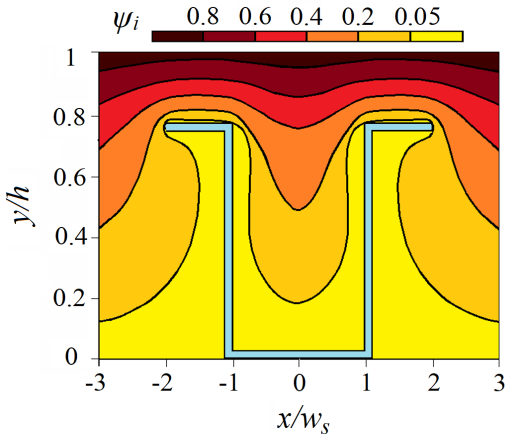

Fig. 7. *Relative temperature changing in thermal insulation layer with hat-stringer inside*

Based on the numerical modelling data, the dependences of the temperature drop on the inner surface of the thermal insulation layer with a hat-stringer inside for different insulation thicknesses and the temperature outside the cabin are plotted (Fig. 8):

$$\psi_w = \frac{(T_w - T_{wn}) - (T_{w0} - T_{wn})}{\Delta T_{wn}}, \qquad (12)$$

where T_{wn} is the scaled temperature of internal layer surfaces; T_{w0} is the surface temperature without the effect of a hat-stringer; $\Delta T_{wn} = T_c - T_{wn}$ is the scaled temperature difference.

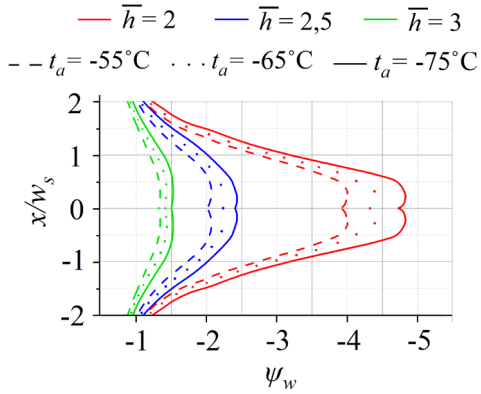

Fig. 8. *Temperature decreasing on internal wall within the area of hat-stringer*

An estimation of the heat properties deterioration of the multilayer wall, associated with the location of a hat-stringer in the thermal insulation layer, was conducted. For this purpose, the effect of the ratio of the thermal insulation size to the size of the stringer, the change in the thermal conductivity coefficient of the thermal insulation was evaluated:

$$\Delta\kappa_i = \frac{(\kappa_i - \kappa_{i0})}{\kappa_{i0}} \cdot 100\ \%, \qquad (13)$$

where κ_{i0} and κ_i are the heat transfer coefficient of the insulation layer without and with a hat-stringer inside. Changing of the heat-transfer coefficient of thermal insulation, conditioned by the hat-stringer, are shown in Fig. 9.

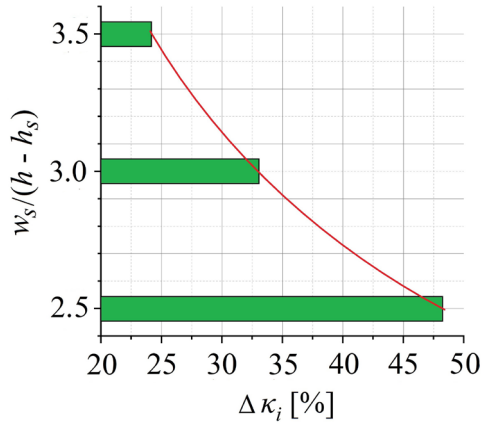

Fig. 9. *Changing of heat transfer coefficient of thermal insulation, conditioned by hat-stringer*

3 CONCLUSIONS

In this article, the results of numerical modelling and evaluation of thermal characteristics of multilayer wall of aircraft cabin with hat-stringer inside are presented. Summarizing the results, it can be concluded that:

1. According to heat transfer modelling through an aircraft cabin wall with an air layer and hat-stringer inside, the evaluation and prediction of thermal characteristics were obtained. As the results of the numerical modelling demonstrate, the thermal resistance of a cabin's multilayer wall does not change with the increase of air layer thickness for more than $2.9 \cdot 10^{-2}$ m.
2. The contribution of the air layer to the overall thermal resistance of the multilayer wall of the aircraft cabin decreases with the increasing emissivity factor of the layer surfaces and equals 20.7 % for $\varepsilon_e = \varepsilon_i = 0.1$ and 8.1% for $\varepsilon_e = \varepsilon_i = 0.9$.
3. The heat changing in the insulation layer with a hat-stringer inside is presented on the grounds of numerical modelling. The modelling results prove that the small thickness of the insulation layer in the area of the hat-stringer in possible minimum temperature contributes to a significant deterioration of thermal resistance in the aircraft multilayer wall, including the rise of the heat transfer coefficient of insulation by more than 47 % and a weighty change in the temperature drop between the internal walls within the area of the insulation layer.

The presented results make it possible to evaluate the thermal characteristics of cabin multilayer walls depending on the material parameters of layers during the rational design creation for the aerial vehicle.

4 ACKNOWLEDGEMENTS

The research described in this paper was financially supported by the National Natural Science Foundation of China (51976201) and the Natural Science Foundation of Zhejiang Province (LY22E06006)

5 REFERENCES

[1] Qu, J., Wang, D., Wang, W., Dang, S. (2022). Study on bidirectional coupling of human thermal comfort parameters and cabin thermal environment. *Journal of System Simulation*, vol. 34, no. 1, p. 20-35, DOI:**10.16182/j.issn1004731x.joss.21-0558**.

[2] Sanchez, F., Liscouet-Hanke, S., Boutin, Y., Beaulac, S., Dufresne, S. (2018). Multi-level modeling methodology for aircraft thermal architecture design. *SAE Technical Paper Series*, 2018-01-1910, **DOI:10.4271/2018-01-1910**.

[3] Duan, X., Yu, S., Chu, J., Chen, D., Su, Z. (2021). CFD-based evaluation of flow and temperature characteristics of airflow in an aircraft cockpit. *Computer Modeling in Engineering & Sciences*, vol. 130, no. 2, p. 701-721, **DOI:10.32604/cmes.2022.016779**.

[4] Wang, J., Xiang, Z. R., Zhi, J. Y., Chen, J. P., He, S. J., Du, Y. (2021). Assessment method for civil aircraft cabin comfort: contributing factors, dissatisfaction indicators, and degrees of influence. *International Journal of Industrial Ergonomics*, vol. 81, p. 103045, **DOI:10.1016/j.ergon.2020.103045**.

[5] Fan, J., Zhou, Q. (2019). A review about thermal comfort in aircraft. *Journal of Thermal Science*, vol. 28, no. 2, p. 169-183, **DOI:10.1007/s11630-018-1073-5**.

[6] Yu, N., Zhang, Y., Zhang, M., Li, H. (2021). Thermal condition and air quality investigation in commercial airliner cabins. *Sustainability*, vol. 13 no. 13, p. 7047, **DOI:10.3390/su13137047**.

[7] Jia, S., Lai, D., Kang, J., Li, J., Liu, J. (2018). Evaluation of relative weights for temperature, CO_2, and noise in the aircraft cabin environment. *Building and Environment*, vol. 131, p. 108-116, **DOI:10.1016/j.buildenv.2018.01.009**.

[8] Cui, W., Wu, T., Ouyang, Q., Zhu, Y. (2017). Passenger thermal comfort and behavior: a field investigation in commercial aircraft cabins. *Indoor Air*, vol. 27, no. 1, p. 94-103, **DOI:10.1111/ina.12294**.

[9] Winzen, J., Marggraf-Micheel, C. (2013). Climate preferences and expectations and their influence on comfort evaluations in an aircraft cabin. *Building and Environment*, vol. 64, p. 146-151, **DOI:10.1016/j.buildenv.2013.03.002**.

[10] Lei, L., Zheng, H., Xue, Y., & Liu, W. (2022). Inverse modeling of thermal boundary conditions in commercial aircrafts based on Green's function and regularization method. *Building and Environment*, vol. 217, p. 109062, **DOI:10.1016/j.buildenv.2022.109062**.

[11] Çiçek, O., & Baytaş, A. C. (2021). Local thermal non-equilibrium conjugate forced convection and entropy generation in an aircraft cabin with air channel partially filled porous insulation. *Aircraft Engineering and Aerospace Technology*, vol. 94, no. 2, p. 210-225, **DOI:10.1108/AEAT-02-2021-0039**.

[12] Dong, L., Chen, X., Wang, Z., & Zhang, Z. (2018). Factors affecting overall and local temperature distribution in aircraft cabins. *Journal of Building Engineering*, vol.18, p. 125-129, **DOI:10.1016/j.jobe.2018.03.013**.

[13] Geron, M., Butler, C., Stafford, J. Newport, D. (2013). Development and validation of a compact thermal model for an aircraft compartment. *Applied Thermal Engineering*, vol. 61, no. 2, p. 65-74, **DOI:10.1016/j.applthermaleng.2013.07.012**.

[14] Butler, C., Newport, D. (2014). Experimental and numerical analysis of thermally dissipating equipment in an aircraft confined compartment. *Applied Thermal Engineering*, vol. 73, no. 1, p. 869-878, **DOI:10.1016/j.applthermaleng.2014.08.035**.

[15] Wanhill, R., Barter, S., Molent, L. (2019). Fokker 100 fuselage test: Lap joints exponential FCG analysis. Fatigue crack growth failure and lifing analyses for metallic aircraft structures and components. *Springer Briefs in Applied Sciences and Technology*, Springer, Dordrecht, **DOI:10.1007/978-94-024-1675-6_9**.

[16] Wu, D., Wang, Y., Gao, Z., Yang, J. (2015). Insulation performance of heat-resistant material for high-speed aircraft under thermal environments. *Journal of Materials Engineering and Performance*, vol. 24, p. 3373-3385, **DOI:10.1007/s11665-015-1626-7**.

[17] Çiçek, O., Baytaş, A.C. (2021). Local thermal non-equilibrium conjugate forced convection and entropy generation in an aircraft cabin with air channel partially filled porous insulation. *Aircraft Engineering and Aerospace Technology*, vol. 94, no. 2, p. 210-225, **DOI:10.1108/AEAT-02-2021-0039**.

[18] Chen, L., Wang, S., Li, G., Lin, C.-H., Zhang, T. T. (2016). CFD modeling of moisture accumulation in the insulation layers of an aircraft. *Applied Thermal Engineering*, vol. 102, p. 1141-1156, **DOI:10.1016/j.applthermaleng.2016.04.048**.

[19] Zhang, T.T., Tian, L., Lin, C.-H., Wang, S. (2012). Insulation of commercial aircraft with an air stream barrier along fuselage. *Building and Environment*, vol. 57, p. 97-109, **DOI:10.1016/j.buildenv.2012.04.013**.

[20] Zhang, Y., Liu, J., Pei, J., Li, J. Wang, C. (2017). Performance evaluation of different air distribution systems in an aircraft cabin mockup. *Aerospace Science and Technology*, vol. 70, p. 359-366, **DOI:10.1016/J.AST.2017.08.009**.

[21] Liu, M., Chang, D., Liu, J., Ji, S., Lin, C.H., Wei, D., Long, Z., Zhang, T., Shen, X., Cao, Q., Li, X. (2021). Experimental investigation of air distribution in an airliner cabin mockup with displacement ventilation. *Building and Environment*, vol. 191, art. ID. 107577, **DOI:10.1016/j.buildenv.2020.107577**.

[22] Minkowycz, W. J., Sparrow, E. M., & Murthy, J. Y. (2006). *Handbook of Numerical Heat Transfer*, John Willey & Sons. Inc., New York.

[23] Patankar, S.V. (2018). Numerical Heat Transfer And Fluid Flow. CRC Press, Boca Raton, **DOI:10.1201/9781482234213**.